Atmos. Chem. Phys. Discuss., 12, 20181–20207, 2012
www.atmos-chem-phys-discuss.net/12/20181/2012/
doi:10.5194/acpd-12-20181-2012

Atmospheric Chemistry and Physics Discussions

Peroxyacetyl nitrate (PAN) and peroxyacetic acid (PAA) measurements by iodide chemical ionisation mass spectrometry: first analysis of results in the boreal forest and implications for the measurement of PAN fluxes

G. J. Phillips[1], N. Pouvesle[1,*], J. Thieser[1], G. Schuster[1], R. Axinte[1], H. Fischer[1], J. Williams[1], J. Lelieveld[1], and J. N. Crowley[1]

[1]Department of Atmospheric Chemistry, Max Planck Institute for Chemistry, Hahn-Meitner Weg 1, 55128 Mainz, Germany
[*]now at: ET Energie Technologie GmBH, Eugen-Sänger-Ring 4, 85649 Brunnthal, Germany

Received: 20 July 2012 – Accepted: 1 August 2012 – Published: 13 August 2012

Correspondence to: G. J. Phillips (gavin.phillips@mpic.de)

Published by Copernicus Publications on behalf of the European Geosciences Union.

Abstract

We describe measurements of peroxyacetyl nitrate ($CH_3C(O)O_2NO_2$, PAN) and peroxyacetic acid ($CH_3C(O)OOH$, PAA) in the Boreal forest using iodide chemical ionization mass spectrometry (ICIMS). The measurements were made during the Hyytiälä United Measurement of Photochemistry and Particles – Comprehensive Organic Particle and Environmental Chemistry (HUMPPA-COPEC-2010) measurement intensive. Mixing ratios of PAN and PAA were determined by measuring the acetate ion signal ($CH_3C(O)O_2^-$, *m/z* 59) resulting from reaction of $CH_3C(O)O_2$ (from the thermal dissociation of PAN) or $CH_3C(O)OOH$ with iodide ions using alternatively heated and ambient temperature inlet lines. During conditions of high temperature and low NO_x, PAA mixing ratios were similar to, or exceeded those of PAN and thus contributed a significant fraction of the total acetate signal. PAA is thus a potential interference for ICIMS measurements of PAN, and especially eddy covariance flux measurements in environments where the PAA flux is likely to be a significant proportion of the short timescale acetate ion variability. Within the range of mixing ratios of NO_x measured during HUMPPA-COPEC, the ratio of PAA-to-PAN was found to be sensitive to temperature (through the thermal decomposition rate of PAN) and the HO_2 mixing ratio, thus providing some constraint to estimates of photochemical activity and oxidation rates in the Boreal environment.

1 Introduction

Acyl peroxy nitric anhydrides ($RC(O)OONO_2$, APNs) are an important class of atmospheric trace species formed via the reaction of NO_2 with acyl peroxy radicals ($RC(O)O_2$), themselves formed from the oxidation and photolysis of volatile organic trace gases (VOCs). APNs have been widely studied owing to their properties as phytotoxic agents and lachrymatory components of air pollution (Stephens et al., 1961). In polluted regions, where ozone production is VOC limited, APNs sequester significant

ACPD
12, 20181–20207, 2012

amounts of NO_x thus increasing the chain length of the HO_x cycle. A further important property of APNs is their thermal instability, leading to short atmospheric lifetimes at high temperatures (1.5 h at 293 K) and moderate to long lifetimes at lower temperatures (50 h at 273 K). This instability allows for the re-release of NO_x and $RC(O)O_2$ far from their source regions making APNs potentially important components of nitrogen deposited in sensitive rural ecosystems (Sparks et al., 2003). The most abundant and most studied of the APNs is acetylperoxy nitric anhydride (peroxyacetyl nitrate, PAN, $CH_3C(O)O_2NO_2$), (e.g. Singh and Hanst, 1981; Singh and Salas, 1983; Singh et al., 1992; Roberts et al., 1998, 2003, 2007; LaFranchi et al., 2009; Fischer et al., 2011). PAN is formed in Reaction (R1) between NO_2 and the acetylperoxy radical $CH_3C(O)O_2$, a radical intermediate in the oxidation of anthropogenic (e.g. propane) and biogenic VOCs (e.g. isoprene and α-pinene, LaFranchi et al., 2010; Atkinson and Arey, 2003; Peeters et al., 2001; Fantechi et al., 2002) as illustrated in Fig. 1.

$$CH_3C(O)O_2 + NO_2 + M \rightarrow CH_3C(O)O_2NO_2 + M \quad \text{(R1)}$$

$$CH_3C(O)O_2NO_2 + M \rightarrow CH_3C(O)O_2 + NO_2 + M \quad \text{(R2)}$$

$$CH_3C(O)O_2 + NO \rightarrow CH_3 + CO_2 + NO_2 \quad \text{(R3)}$$

PAN is long-lived with respect to reaction with OH ($\sim$ 1 yr at $[OH] = 1 \times 10^6$ molecule cm^{-3}) or photolysis (30 days) and its lifetime in the boundary layer (Talukdar et al., 1995) is controlled by thermal decomposition (in the presence of $CH_3C(O)O_2$ scavengers such as NO in R3) and by transport and deposition. The acetylperoxy radical is permanently removed in reaction with NO whereby the carbonyl functionality ends up as CO_2 via decomposition of the intermediate CH_3CO_2 alkoxy radical (not shown).

Figure 1 also indicates that peroxyacetic acid, PAA is formed in the competitive Reaction (R4a) of the $CH_3C(O)O_2$ radicals with HO_2. The formation of PAA in Reaction (R4a) represents just one channel of this reaction with (R4b) and (R4c) also contributing significantly (Dillon and Crowley, 2008; Taraborrelli et al., 2012):

$$CH_3C(O)O_2 + HO_2 \rightarrow CH_3C(O)OOH + O_2 \quad \text{(R4a)}$$

ACPD
12, 20181–20207, 2012

$\rightarrow CH_3C(O)OH + O_3$ (R4b)

$\rightarrow OH + CH_3 + O_2 + CO_2$ (R4c)

Under most atmospheric conditions, the rate coefficients for reaction of $CH_3C(O)O_2$ with NO_2 and HO_2 are similar (k_1 and k_3 at 298 K and 1 bar pressure are 9.3×10^{-12} and 1.4×10^{-11} cm^3 $molecule^{-1}$ s^{-1}, respectively) and the relative flux of $CH_3C(O)O_2$ radicals into the PAN and PAA forming channels will depend on the relative abundance of NO_2 and HO_2, which, apart from extremely clean low-NO_x environments (when $[HO_2] > [NO_2]$) will generally favour PAN. However, as stated above, in the summertime boundary layer, PAN is short lived and will readily decompose to $CH_3C(O)O_2$, implying that the formation of the thermally stable peroxyacid will be a significant $CH_3C(O)O_2$ sink in warm conditions with reasonably low NO_x levels, e.g. as encountered during HUMPPA-COPEX 2010 (see later). The lifetime of PAA with respect to photolysis is several weeks and (in the absence of a measurement of the rate coefficient) estimates of its lifetime due to reaction with OH are between 2 and 12 days (Orlando and Tyndall, 2003) reforming $CH_3C(O)O_2$ (R5).

$CH_3C(O)OOH + OH \rightarrow CH_3C(O)O_2 + H_2O$ (R5)

With a moderate solubility (measurements vary between 670 and 840 M atm^{-1} at 298 K, Sander, 1997) the boundary layer lifetime of PAA will also be partially determined by deposition, especially in forested regions. Similar to the role NO in (R3), PAA formation can thus be considered an indirect sink for PAN as it drains $CH_3C(O)O_2$ radicals from the equilibrium between (R1) and (R2).

In the absence of a direct, biogenic emission, the PAA mixing ratio can be an important indicator of photochemical activity and (at low NO_x) acts as a sink for both $CH_3C(O)O_2$ and HO_2. Despite this, field measurements of PAA (sometimes measured alongside other organic peroxides with HPLC) are few and far between (Fels and Junkermann, 1994; Zhang et al., 2010; He et al., 2010), though chemical ionisation mass spectrometry using CF_3O^- ions appears to be a promising new technique (Crounse et al., 2006).

ACPD
12, 20181–20207, 2012

A recent development in PAN measurements has been the use of iodide ion mass spectrometry (Slusher et al., 2004) which uses the thermal instability of PAN and the reaction of $CH_3C(O)O_2$ with I^- to generate the acetate ion, $CH_3CO_2^-$, which is detected at $m/z = 59$:

$$CH_3C(O)O_2 + I^- \rightarrow CH_3CO_2^- + IO \quad \text{(R6)}$$

This technique has been used to make measurements with high sensitivity and at high time resolution (Wolfe et al., 2007; LaFranchi et al., 2010; Roiger et al., 2011) e.g. for use in eddy correlation studies of PAN deposition (Turnipseed et al., 2006; Wolfe et al., 2009). Whilst calibration and air-matrix artefacts associated with the measurement of PAN (and other APNs) with this technique have received some attention (Zheng et al., 2011; Mielke and Osthoff, 2012a) here we focus on the discovery that PAA is also converted to the acetate ion via reaction with I^- and, when attempting to measure PAN, represents a non-trivial source of acetate ion signal both in terms of magnitude and variability. We present a dataset of quasi-simultaneous PAN and PAA measurements made during the HUMPPA-COPEC campaign and also note the potential pitfalls when attempting measurements of PAN fluxes in similar environments. We also emphasise the positive aspects of the accidental discovery during HUMPPA-COPEC-2010 that PAA can be sensitively and rapidly detected using the ICIMS method, and using a preliminary analysis, indicate how PAA and PAN measurements together can give new insight into photo-oxidation processes in the low and high NO_x regimes.

2 Methods

2.1 HUMPPA-COPEC site and ancillary measurements

The measurements presented in this paper were made as part of the summertime boreal forest measurement intensive (HUMPPA-COPEC-2010). The field site and the majority of variable measured during the intensive are described in detail by Williams

ACPD
12, 20181–20207, 2012

et al. (2011). The HUMPPA-COPEC measurement tower, operated by the University of Helsinki, was located at the SMEAR II-Hyytiälä station within the boreal forest (latitude 61°51′ N; longitude 24°17′ E). The forest surrounding the site was dominated by a mixture of coniferous forest (Scots pine (*Pinus silvestris L.*) and Norway spruce (*Picea abies L.*)) and mixed forest (conifers and Silver birch (*Betula pendula Roth*)). The measurement tower was situated on the edge of a small clearing, approximately 20 m in diameter, within the surrounding forest.

2.2 Instrumentation

2.2.1 PAN and PAA via ICIMS

The CIMS instrument was constructed by THS Instruments, Georgia, USA and is based on the thermal dissociation-CIMS instrument described by (Slusher et al., 2004) and (Zheng et al., 2011) with minor differences. The instrument includes four components: Thermal dissociation (TD), ion-molecule reactor (IMR), collisional de-clustering (CDC), and mass selection (QMA). The thermal dissociation region consists of a 15 cm section of Teflon tube (PFA) heated to a temperature of 423 K measured on the external surface of the tube by a thermocouple. Laboratory characterization of the inlet showed this temperature to give the best yield of $CH_3CO_2^-$ ions for a constant flow of PAN (Fig. 2a). The temperature of the gas flowing through the inlet was not determined.

The heated PFA tube is attached in front of an orifice leading to the IMR. The orifice size is adjustable and a pressure of 21 Torr is maintained within the IMR independent of the external pressure. A flow of 1 l (STD) min^{-1} of N_2 and CH_3I is added to the IMR via a Po-210 radioactive source generating iodide ions. The sample passes through a second pinhole to the collisional dissociation chamber (CDC) for the minimization of ion clusters before finally entering an octopole ion guide and the quadrupole mass analyser (QMA).

The background is determined by diverting the inlet flow through a 30 cm section of metal tubing heated to 473 K and filled with steel wool to destroy any analyte in the

ACPD
12, 20181–20207, 2012

flow. The instrument was calibrated on-line using a photochemical PAN source similar to that described by Warneck and Zerbach (1992) which was continuously operated and switched into the zero air flow during calibration periods every hour. The effect of artefacts resulting from the photolysis of acetone in the source was accounted for by measuring the response to the source with an ambient temperature inlet and subtracting any subsequent signal. The photochemical PAN source was calibrated prior to and during the campaign using thermal-dissociation cavity ring-down spectroscopy (TD-CRDS) in a similar manner to described in Furgeson et al. (2011).

The sample inlet was situated on the main HUMPPA-COPEC instrument tower, a height of 20 m above the ground at approximately the same height as the surrounding tree canopy. The sampling line consisted of ~30 m of 1/4″ OD, PFA tubing which was maintained at about 30 °C. The sample was drawn down the tubing at a flowrate of 6 l (STD) min^{-1} resulting in a residence time of approximately 1 s. The sample line was not characterized for loss of PAN or PAA.

During the campaign setup phase the instrument was sporadically operated without heating the thermal dissociation region (precluding detection of PAN) and an ambient signal at $m/z = 59$ was recorded which revealed high temporal variability. We determined that this signal was likely due to the presence of PAA and the instrument was subsequently operated with an alternating heated and ambient temperature cycle for the thermal dissociation region.

As we had not anticipated detection of PAA, the ICIMS sensitivity and its dependence of humidity was determined post-campaign. A PAA standard was produced by sampling the dynamically diluted head space of a sample of 40 % PAA in acetic acid simultaneously with the iodide CIMS and an ROOH instrument, described below. The small interference from acetic acid in the standard was removed by using a pure acetic acid standard, recording mass scans and calculating the signal ratio of m/z 187 : 59 ($CH_3C(O)OHI^-$: $CH_3C(O)O^-$). A multipoint calibration was performed and the CIMS sensitivity to PAA was determined to be 5.7 Hz pptv^{-1} at 290 K and RH of 1 % at 760 Torr and 26 °C. The detection sensitivity was found to be non monotonically dependent

ACPD
12, 20181–20207, 2012

on the absolute humidity (Fig. 2c) and the raw data was corrected for the relevant range of humidity measured during HUMPPA-COPEC 2010. The dependence of the PAN detection sensitivity on humidity was also determined and found to be relatively weak for the range of humidity encountered during the campaign (Fig. 2b). The weak, positive dependence on humidity at RH values between ~10 and ~60 % is very similar to that observed previously for PAN detection via ICIMS (Slusher et al., 2004; Zheng et al., 2011). The detection of PAA at *m/z* 59 presumably occurs via abstraction at the weak O-OH bond of the peroxy acid, with reaction enthalpy of $-78\,\mathrm{kJ\,mol^{-1}}$:

$$CH_3C(O)OOH + I^- \rightarrow CH_3CO_2^- + HOI \quad \text{(R7)}$$

with the resulting acetate ion being detected (Furgeson et al., 2011; Mielke and Osthoff, 2012b). The fact that the signal is reduced at very low RH suggests that the dominant ionizing ion is in fact $I^-(H_2O)_n$ as for PAN.

Reasons for the complex RH dependence of the *m/z* signal due to PAA are not completely clear; however some initial investigations have been completed. Tests with the calibration standard indicate that at high humidities, water-acetate clusters are produced in the IMR ($(H_2O)_nCH_3C(O)O^-$, where n = 0, 2 and 1 in order of decreasing abundance). When sufficient potential is applied in the CDC, these ions are likely to be detected at n = 0, i.e. *m/z* 59. However, at low declustering energies (and sufficient RH) PAA is also detected at *m/z* 203 and 221 corresponding to the ions $CH_3C(O)OOHI^-$ and $(H_2O)CH_3C(O)OOHI^-$. These signals dramatically decrease and in the case of *m/z* 221 disappear when the instrument is operated using the normal declustering potentials. It is therefore possible that the negative humidity dependence at RH > 2 % is due to the increased number of $(H_2O)_nCH_3C(O)OOHI^-$ formed at high humidity which are subsequently removed in the declustering region and fail to form the acetate ion and thus not detected at *m/z* 59. Alternatively, further reactions in the IMR of $(H_2O)_nCH_3C(O)OOHI^-$ with H_2O which do not lead (after declustering) to $CH_3C(O)OO^-$ would also lead to a complex dependence on RH as observed.

The PAA sensitivity at *m/z* 59 is about 2.5 times less than that for PAN at low humidity. Although this value was obtained under the same mass spectrometer operating

ACPD
12, 20181–20207, 2012

conditions, we recognise that post-campaign calibration is non-ideal and the error associated with the PAA measurement is adjusted accordingly. As loss of the $CH_3C(O)O_2$ radical in passing through the TD region and into the IMR is expected to be significant compared to PAA, the relative rate constant k_6/k_7 is expected to be significantly less than 2.5.

Although not calibrated, several other mass-to-charge ratios (m/z = 73, 85, 87) were monitored when the inlet was not heated, and these are assigned to further peracids i.e. permethacrylic acid (PMA), perpropanoic acid and perbutanoic acid formed in competition to the APN at higher NO_x levels and lower temperatures. Raw count rates for the unheated period reached a maximum of 50 % of the gross heated inlet signal for m/z 85 and 87, and 30 % of the gross heated inlet signal for m/z 73.

The signal due to the sum of PAN + PAA (hot inlet) was monitored continuously and the inlet was cooled to ambient temperature for 10 min once an hour to determine the concentration of PAA. The signal due to PAA was linearly interpolated and subtracted from the PAA + PAN signal to give the signal due to PAN.

In addition to "interference" at m/z = 59 due to the direct sensitivity to PAA described here, APN detection using TD-ICIMS suffers from known matrix effects via reactions of NO_x and organic acids. Mielke and Osthoff (2012b) have shown that high NO_x conditions can result in a significant negative bias on the detection of PANs, particularly the higher PANs (e.g. MPAN, APAN) via the reaction of NO or NO_2 with the $RC(O)O_2$ radical fragment within the TD region. Acetate anions formed from the $CH_3C(O)O_2 + I^-$ chemistry (R6) can undergo further charge transfer resulting in spurious signals at mass-to-charge ratios corresponding to higher APNs resulting in their overestimation and a decrease in the signal for PAN itself. During HUMPPA-COPEC NO_x levels were low (always less than 1 ppb, generally less than 200 pptv) and NO_x related biases on our PAN measurements are negligible.

ACPD
12, 20181–20207, 2012

2.2.2 Organic peroxides

Mixing ratios of hydrogen peroxide (H_2O_2) and total organic peroxides (ROOH) were measured in-situ using a modified commercial instrument (Model AL2021, Aero-Laser GmbH, Garmisch-Partenkirchen, Germany) based on the horseradish peroxidase/catalase/p-hydroxypenyl acetic acid wet chemical fluorescence measurement technique described by (Lazrus et al., 1986). The operation of two channels allows the quantification of H_2O_2, and an estimate of total organic hydroperoxides (ROOH) can be made assuming an average efficiency of detection (related to solubility) for the organic peroxides. For the calibration of the ICIMS sensitivity to PAA, zero measurements and liquid calibrations of H_2O_2 were performed to quantify instrument drifts. Gas calibrations were made using a H_2O_2 permeation source to estimate the inlet efficiency for H_2O_2. A stripping efficiency for PAA was measured as 90 (±5) % which is consistent with calculations using Henry's law.

3 Results and discussion

3.1 PAN and PAA

The time series of PAN and PAA for the HUMPPA-COPEC campaign are shown in Fig. 3. The data indicate the expected correlation between two trace-gases with a common radical source ($CH_3C(O)O_2$) with maximum mixing ratios of about 1.2 ppbv for PAA and 800 pptv for PAN. Although the PAN mixing ratio usually exceeded that of PAA, on four occasions, all marked by temperatures above the campaign average (22.07, 26.7, 28–29.07 and 08.08) the PAA mixing ratio was larger. Also shown in this figure is a time series of total organic peroxides, which are clearly correlated very closely with PAA, although the absolute contribution of PAA to the total organic peroxide budget is difficult to determine owing to the reliance of the total organic peroxide measurement

ACPD
12, 20181–20207, 2012

on an assumed combination of detection efficiencies corresponding to the individual contribution of each organic peroxide to the total signal.

On some occasions, usually at nighttime when relative humidity increased or during rainy or misty periods, the PAA mixing ratio was dramatically reduced due to efficient wet and/or dry deposition onto moist surfaces. This observation, typical of a soluble species, and the obvious correlation with the ROOH data provided early clues to help identify the source of the signal at $m/z = 59$ when operating the cold inlet.

The largest mixing ratios of both PAN and PAA were observed during the period 26–30 July, in which the highest temperatures ($> 30\,^{\circ}$C) were recorded. At the largest temperatures encountered during the campaign, the lifetime of PAN with respect to thermal dissociation was of the order of only 20 min. Under such conditions, PAN can be considered to have been locally generated and is not being transported to the site from distant pollution sources.

Figure 4 shows the average diurnal mixing ratios of PAN and PAA for the whole campaign, as well as the temperature and the PAA-to-PAN ratio. Average mixing ratios of PAN ranged between 150 pptv at 03:30 and a maximum of 300 pptv at 12:30 (times are UTC +2) with a range of approximately 100–150 pptv between the 25th and 75th percentile of the data. The average concentrations of PAA ranged between 60 pptv, at 04:30, and 280 pptv, at 13:30, with a variable range of a few tens of pptv at night to 300 pptv between the 25th and 75th percentile during the middle of the day. The average PAA diurnal profile is more modulated that that of PAN and PAA is clearly lost more rapidly at night. This observation is consistent with the relative solubility (PAA/PAN) of > 100 (Sander, 1997) resulting in more efficient deposition to the canopy due to its radiative cooling after sunset, which promotes the condensation of atmospheric moisture.

The lowermost panel of Fig. 4 plots the average PAA-to-PAN ratio, which varies between 0.4 in the early morning, at the lowest temperatures, and reaches a maximum of 1.0 in the mid-afternoon. This ratio closely tracks the average daily variation in temperature and is largely driven by the PAN thermal decomposition rate.

ACPD
12, 20181–20207, 2012

This is understood when we examine the production and loss processes which determine the PAN and PAA mixing ratios. Assuming that both PAA and PAN acquire stationary state concentrations determined by the production terms in 1 and 3 and that PAN is lost by thermal decomposition (2) and deposition and PAA is lost by reaction with OH and deposition we can show that the PAA/PAN ratio is given by:

$$\frac{\mathrm{PAA}}{\mathrm{PAN}} = \frac{[\mathrm{HO_2}]}{[\mathrm{NO_2}]} \cdot \frac{k_{4a}\,(k_2 + D_{\mathrm{PAN}})}{k_1\,(k_5\,[\mathrm{OH}] + \mathrm{D_{PAA}})} \tag{1}$$

where $[HO_2]$ and $[NO_2]$ are the concentrations of HO_2 and NO_2, k_i are rate coefficients for reactions R_i, and D_{PAN} and D_{PAA} are first-order loss terms for deposition of PAN and PAA. Under the warm conditions of this campaign, the thermal deposition rate dominates over the deposition loss term for PAN and this expression simplifies to:

$$\frac{\mathrm{PAA}}{\mathrm{PAN}} = \frac{[\mathrm{HO_2}]}{[\mathrm{NO_2}]} \cdot \frac{k_{4a} k_2}{k_1\,(k_5\,[\mathrm{OH}] + D_{\mathrm{PAA}})} \tag{2}$$

Values of k_1 and k_2, the PAN formation and decomposition rate coefficients, are quite well known, the latter being strongly temperature dependent with k_2 proportional to $\exp(-13000/T)$ (Atkinson et al., 2004). Whilst kinetic data for the overall reaction k_4 are well known, the branching ratio to PAA is uncertain (Atkinson et al., 2006). There are also no experimental determinations of k_5, though, as mentioned above, a rate coefficient close to $10^{-12}\,\mathrm{cm^3\,molecule^{-1}\,s^{-1}}$ seems reasonable and would result in lifetimes which are comparable to those due to dry deposition (i.e. $k_5[\mathrm{OH}] \sim \mathrm{D_{PAA}}$) (Baer et al., 1992). This simple equation indicates that, for a given temperature, the PAA-to-PAN ratio is determined by the HO_2 to NO_2 ratio.

Figure 5 displays the PAA-to-PAN ratio plotted against temperature during the hours of sunlight. The solid lines are calculations of the ratio from Eq. (2) over the campaign temperature range. Recommended kinetic parameters (k_1, k_2, k_{4a}) were taken where available, k_5 was fixed independent of temperature at $3 \times 10^{-12}\,\mathrm{cm^3\,molecule^{-1}\,s^{-1}}$.

ACPD
12, 20181–20207, 2012

The HO_2 mixing ratio (30 pptv) and the PAA deposition rate ($D_{PAA} = 5 \times 10^{-6}\,s^{-1}$ corresponding to a deposition velocity of $0.5\,cms^{-1}$ in a 1 km high BL) were adjusted as representative of the dataset. Note the non-linear response of the PAA/PAN ratio with temperature (driven by the exponential dependence of k_2 on temperature) and the weaker dependence on NO_x variations is semi-quantitatively captured by this simple calculation.

While it is evident that the assumptions within the steady-state approximation are not strictly valid, and that a single, time invariant value for the HO_2 mixing ratio and the deposition velocity of PAA are simplifying estimates, the relationship between PAA and PAN in the conditions encountered during HUMPPA-COPEC, namely low NO_x and high temperatures, give us a valuable insight into the relative importance of HO_2 and NO_x in the dataset and can, to some extent at least, allow one to place a boundary on the HO_2 present at the site. This aspect of the PAA/PAN measurements will be examined in a later publication in a more rigorous examination of the photochemistry of this site, including comparison to measured radical concentrations.

Three other acylperoxynitrate-peroxy acid pairs were monitored during HUMPPA-COPEC. Mass-to-charge ratios 73, 85 and 87, corresponding to PPN, MPAN and PBN, were all measured and found to have significant interferences from their corresponding acid. Figure 6 shows the relationship between PAA and each of three other peracids assuming the same instrument sensitivity as for PAA. The campaign average contribution and range (25th and 75th percentiles), in units of raw signal, of the peracid signal to the total signal (acylperoxynitrate + peroxy acid) for each *m/z* was 31 % (21–47) for *m/z* 73, 76 % (58–100) for *m/z* 85, and 59 % (41–80) for *m/z* 87.

3.2 Implications for the measurement of speciated PAN fluxes by EC-CIMS

The detection of peracids as a significant proportion of the signal measured at the carboxylate mass-to-charge ratios using iodide CIMS has implications for PAN measurements using TD-ICIMS. Not all instruments are necessarily equally sensitive to PAA;

ACPD
12, 20181–20207, 2012

however, these measurements raise an important issue when attempting to measure PANs with TD-ICIMS in environments in which peracids may be reasonably expected.

When measuring PAN concentrations it is possible to avoid artefacts from PAA by either using the addition of NO for the analytical zero, or by measuring the zero without a heated TD region. The addition of NO removes the PA radical formed within the TD region but does not remove PAA and thus signal due to PAA is removed by subtraction. With no heated region, PAN does not dissociate leaving only PAA available for detection. The effectiveness of either of the above methods of correction depends on the variability of PAA, the frequency of the zero, and the relative contribution of PAA to the acetate ion signal.

The correction of EC flux measurements is more problematic. The turbulent flux of scalar components can be measured as the covariance between the concentration of the scalar and the vertical wind component, which in practice is achieved via rapid measurements of vertical wind velocity and the concentration scalar (Kaimal and Finnegan, 1994). If the variability of the scalar is dependent on an artefact in addition to the variable of interest, the flux must be corrected by the flux of the artefact and cannot be removed by the zeroing methods described above. For the specific case of PAN and PAA, it is likely that PAA would exhibit larger deposition velocities than PAN owing to its much greater solubility and relatively high reactivity (e.g. Baer et al., 1992). It is likely therefore that variability detected in the acetate ion using TD-ICIMS will have a significant contribution from PAA and therefore require correction before the promulgation of PAN fluxes.

A number of studies have reported fluxes of PAN using Eddy correlation and the ICIMS technique (Turnipseed et al., 2006; Wolfe et al., 2009; Min et al., 2012). Turnipseed et al. (2006), in a study of PAN fluxes above loblolly pine, found that their measured deposition velocities were larger than were predicted by models and that PAN deposition velocities were increased in wet conditions, consistent with possible contamination of the PAN flux by PAA sensitivity. The data in Turnipseed et al. (2006) have been used to assess the ability of two community models (WRF-Chem dry depo-

ACPD
12, 20181–20207, 2012

sition module (WDDM) and Noah-gas exchange model (Noah-GEM)) to simulate the dry deposition velocities of PAN (Wu et al., 2012). The authors found that both models underestimate the measured deposition velocities, by a factor of 5 for WDDM and 1.6 for Noah-GEM. The discrepancy between the simulation results and the measurements reached a maximum during wet periods.

In measurements above *Pinus ponderosa L.* at Blodgett forest, Wolfe et al. (2009) measured PAN fluxes via eddy correlation using TD-ICIMS in a similar environment to this study. It is likely that the PAA concentration was significant; however, the authors note that they checked the background of the signal with a cool inlet and that it was very low. In our dataset the signal from PAA was very variable and it is possible that this artefact was only sporadically present during the latter study; however the authors do not state the frequency of their cold-inlet checks. Wolfe et al. (2009) do not report PAN deposition velocities during wet conditions owing to the malfunctioning of the sonic anemometer and so any inference of a soluble component of the flux was not possible.

Min et al. (2012), also measuring in Blodgett forest, present a comparison of ΣPN fluxes by EC-TD-LIF (Farmer et al., 2006) with measurements of speciated peroxynitrates fluxes by EC-TD-CIMS. A 30–60 % discrepancy was observed between the two techniques, which was proposed to be due to the formation of peroxynitrates other than the ones measured by the CIMS in the study. An alternative explanation is that the CIMS used is sensitive to PAA and its homologues. It may be possible to use the Min et al. (2012) study to retrospectively determine the flux of PAA using the flux of ΣPN from TD-LIF to correct the TD-ICIMS data.

It is difficult to assess the particular consequences of the detection of PAA fluxes as an artefact of the determination of PAN fluxes in each case owing to the complex interaction of in-canopy chemistry, unknown ambient fluxes of PAA, combined with unknown instrument PAA sensitivities.

ACPD
12, 20181–20207, 2012

4 Conclusions

We present measurements of PAN and PAA using ICIMS by monitoring the acetate ion (*m/z* 59) signal using an alternating heated and ambient temperature inlet system. Concentrations of PAA and PAN were, on average, very similar varying between 100 to 300 pptv, with the ratio of PAA-to-PAN varying, on average, between 0.4 early in the morning up to 1.0 in the mid-afternoon. The PAA-to-PAN ratio is controlled strongly by temperature in these low NO_x conditions and analysis of the steady-state relationship of the two compounds allows, with some assumptions, determination of the relationship between NO_2 and HO_2. PAA is a large proportion of the total signal at *m/z* 59, in our system, and interferes with measurements of PAN unless corrected, in the case of concentration measurements, by frequent instrument zeros by NO addition or inlet heater cycling. Correction of fluxes measured via the eddy covariance technique is more complex and the flux of PAA will need to be determined to correct the flux of PAN. It is very possible that previously published deposition velocities of PAN by TD-ICIMS are enhanced by PAA measured as an artefact.

Acknowledgements. The authors are grateful for the support of the Hyytiälä site engineers and staff. Support of the European Community – Research Infrastructure Action under the FP6 "Structuring the European Research Area" Programme, EUSAAR Contract No. RII3-CT-2006-026140 is gratefully acknowledged.

The service charges for this open access publication
have been covered by the Max Planck Society.

References

Atkinson, R. and Arey, J.: Gas-phase tropospheric chemistry of biogenic volatile organic compounds: a review, Atmos. Environ., 37, S197–S219, 2003.

Atkinson, R., Baulch, D. L., Cox, R. A., Crowley, J. N., Hampson, R. F., Hynes, R. G., Jenkin, M. E., Rossi, M. J., and Troe, J.: Evaluated kinetic and photochemical data for at-

ACPD
12, 20181–20207, 2012

mospheric chemistry: Volume I – gas phase reactions of O_x, HO_x, NO_x and SO_x species, Atmos. Chem. Phys., 4, 1461–1738, doi:10.5194/acp-4-1461-2004, 2004.

Atkinson, R., Baulch, D. L., Cox, R. A., Crowley, J. N., Hampson, R. F., Hynes, R. G., Jenkin, M. E., Rossi, M. J., Troe, J., and IUPAC Subcommittee: Evaluated kinetic and photochemical data for atmospheric chemistry: Volume II – gas phase reactions of organic species, Atmos. Chem. Phys., 6, 3625–4055, doi:10.5194/acp-6-3625-2006, 2006.

Crounse, J. D., McKinney, K. A., Kwan, A. J., and Wennberg, P. O.: Measurement of gas-phase hydroperoxides by chemical ionization mass spectrometry, Anal. Chem., 78, 6726–6732, 2006.

Dillon, T. J. and Crowley, J. N.: Direct detection of OH formation in the reactions of HO_2 with $CH_3C(O)O_2$ and other substituted peroxy radicals, Atmos. Chem. Phys., 8, 4877–4889, doi:10.5194/acp-8-4877-2008, 2008.

Fantechi, G., Vereecken, L., and Peeters, J.: The OH-initiated atmospheric oxidation of pinonaldehyde: detailed theoretical study and mechanism construction, Phys. Chem. Chem. Phys., 4, 5795–5805, doi:10.1039/b205901k, 2002.

Farmer, D. K., Wooldridge, P. J., and Cohen, R. C.: Application of thermal-dissociation laser induced fluorescence (TD-LIF) to measurement of HNO_3, Σalkyl nitrates, Σperoxy nitrates, and NO_2 fluxes using eddy covariance, Atmos. Chem. Phys., 6, 3471–3486, doi:10.5194/acp-6-3471-2006, 2006.

Fels, M. and Junkermann, W.: The occurrence of organic peroxides in air at a mountain site, Geophys. Res. Lett., 21, 341–344, doi:10.1029/93gl01892, 1994.

Fischer, E. V., Jaffe, D. A., and Weatherhead, E. C.: Free tropospheric peroxyacetyl nitrate (PAN) and ozone at Mount Bachelor: potential causes of variability and timescale for trend detection, Atmos. Chem. Phys., 11, 5641–5654, doi:10.5194/acp-11-5641-2011, 2011.

Furgeson, A., Mielke, L. H., Paul, D., and Osthoff, H. D.: A photochemical source of peroxypropionic and peroxyisobutanoic nitric anhydride, Atmos. Environ., 45, 5025–5032, doi:10.1016/j.atmosenv.2011.03.072, 2011.

He, S. Z., Chen, Z. M., Zhang, X., Zhao, Y., Huang, D. M., Zhao, J. N., Zhu, T., Hu, M., and Zeng, L. M.: Measurement of atmospheric hydrogen peroxide and organic peroxides in beijing before and during the 2008 olympic games: chemical and physical factors influencing their concentrations, J. Geophys. Res.-Atmos., 115, D17307, doi:10.1029/2009jd013544, 2010.

ACPD
12, 20181–20207, 2012

Kaimal, J. C. and Finnegan, J. J.: Atmospheric Boundary Layer Flows, Oxford University Press, NY, USA, 1994.

LaFranchi, B. W., Wolfe, G. M., Thornton, J. A., Harrold, S. A., Browne, E. C., Min, K. E., Wooldridge, P. J., Gilman, J. B., Kuster, W. C., Goldan, P. D., de Gouw, J. A., McKay, M., Goldstein, A. H., Ren, X., Mao, J., and Cohen, R. C.: Closing the peroxy acetyl nitrate budget: observations of acyl peroxy nitrates (PAN, PPN, and MPAN) during BEARPEX 2007, Atmos. Chem. Phys., 9, 7623–7641, doi:10.5194/acp-9-7623-2009, 2009.

Lazrus, A. L., Kok, G. L., Lind, J. A., Gitlin, S. N., Heikes, B. G., and Shetter, R. E.: Automated fluorometric method for hydrogen-peroxide in air, Anal. Chem., 58, 594–597, doi:10.1021/ac00294a024, 1986.

Mielke, L. H. and Osthoff, H. D.: On quantitative measurements of peroxycarboxylic nitric anhydride mixing ratios by thermal dissociation chemical ionization mass spectrometry, Int. J. Mass Spectrom., 310, 1–9, doi:10.1016/j.ijms.2011.10.005, 2012.

Min, K.-E., Pusede, S. E., Browne, E. C., LaFranchi, B. W., Wooldridge, P. J., Wolfe, G. M., Harrold, S. A., Thornton, J. A., and Cohen, R. C.: Observations of atmosphere-biosphere exchange of total and speciated peroxynitrates: nitrogen fluxes and biogenic sources of peroxynitrates, Atmos. Chem. Phys. Discuss., 12, 6205–6233, doi:10.5194/acpd-12-6205-2012, 2012.

Orlando, J. J. and Tyndall, G. S.: Gas phase uv absorption spectra for peracetic acid, and for acetic acid monomers and dimers, J. Photochem. Photobio. A, 157, 161–166, 2003.

Peeters, J., Vereecken, L., and Fantechi, G.: The detailed mechanism of the OH-initiated atmospheric oxidation of α-pinene: a theoretical study, Phys. Chem. Chem. Phys., 3, 5489–5504, 2001.

Roberts, J. M., Williams, J., Baumann, K., Buhr, M. P., Goldan, P. D., Holloway, J., Hubler, G., Kuster, W. C., McKeen, S. A., Ryerson, T. B., Trainer, M., Williams, E. J., Fehsenfeld, F. C., Bertman, S. B., Nouaime, G., Seaver, C., Grodzinsky, G., Rodgers, M., and Young, V. L.: Measurements of PAN, PPN, and MPAN made during the 1994 and 1995 nashville intensives of the Southern oxidant study: Implications for regional ozone production from biogenic hydrocarbons, J. Geophys. Res.-Atmos., 103, 22473–22490, doi:10.1029/98jd01637, 1998.

Roberts, J. M., Jobson, B. T., Kuster, W., Goldan, P., Murphy, P., Williams, E., Frost, G., Riemer, D., Apel, E., Stroud, C., Wiedinmyer, C., and Fehsenfeld, F.: An examination of the chemistry of peroxycarboxylic nitric anhydrides and related volatile organic compounds dur-

ACPD
12, 20181–20207, 2012

ing texas air quality study 2000 using ground-based measurements, J. Geophys. Res., 108, 4495, doi:10.1029/2003jd003383, 2003.
Roberts, J. M., Marchewka, M., Bertman, S. B., Sommariva, R., Warneke, C., de Gouw, J., Kuster, W., Goldan, P., Williams, E., Lerner, B. M., Murphy, P., and Fehsenfeld, F. C.: Measurements of pans during the new england air quality study 2002, J. Geophys. Res.-Atmos., 112, D20306, doi:10.1029/2007jd008667, 2007.
Roiger, A., Aufmhoff, H., Stock, P., Arnold, F., and Schlager, H.: An aircraft-borne chemical ionization – ion trap mass spectrometer (CI-ITMS) for fast PAN and PPN measurements, Atmos. Meas. Tech., 4, 173–188, doi:10.5194/amt-4-173-2011, 2011.
Sander, R.: Compilation of Henry's Law Constants for Inorganic and Organic Species of Potential Importance in Environmental Chemistry, available at: http://www.rolf-sander.net/henry/henry.pdf, last access: 12 August 2012, 1997.
Singh, H. B. and Hanst, P. L.: Peroxyacetyl nitrate (PAN) in the unpolluted atmosphere – an important reservoir for nitrogen-oxides, Geophys. Res. Lett., 8, 941–944, doi:10.1029/GL008i008p00941, 1981.
Singh, H. B. and Salas, L. J.: Peroxyacetyl nitrate in the free troposphere, Nature, 302, 326–328, doi:10.1038/302326a0, 1983.
Singh, H. B., Ohara, D., Herlth, D., Bradshaw, J. D., Sandholm, S. T., Gregory, G. L., Sachse, G. W., Blake, D. R., Crutzen, P. J., and Kanakidou, M. A.: Atmospheric measurements of peroxyacetyl nitrate and other organic nitrates at high-latitudes – possible sources and sinks, J. Geophys. Res.-Atmos., 97, 16511–16522, 1992.
Slusher, D. L., Huey, L. G., Tanner, D. J., Flocke, F. M., and Roberts, J. M.: A thermal dissociation-chemical ionization mass spectrometry (TD-CIMS) technique for the simultaneous measurement of peroxyacyl nitrates and dinitrogen pentoxide, J. Geophys. Res.-Atmos., 109, D19315, doi:10.1029/2004JD004670, 2004.
Sparks, J. P., Roberts, J. M., and Monson, R. K.: The uptake of gaseous organic nitrogen by leaves: a significant global nitrogen transfer process, Geophys. Res. Lett., 30, 2189, doi:10.1029/2003gl018578, 2003.
Stephens, E. R., Darley, E. F., Taylor, O. C., and Scott, W. E.: Photochemical-reaction products in air-pollution, International Journal of Air and Water Pollution, 4, 79–100, 1961.
Talukdar, R. K., Burkholder, J. B., Schmoltner, A. M., Roberts, J. M., Wilson, R. R., and Ravishankara, A. R.: Investigation of the loss processes for peroxyacetyl nitrate in the atmo-

ACPD
12, 20181–20207, 2012

sphere: UV photolysis and reaction with OH, J. Geophys. Res.-Atmos., 100, 14163–14173, doi:10.1029/95jd00545, 1995.
Taraborrelli, D., Lawrence, M. G., Crowley, J. N., Dillon, T. J., Gromov, S., Groß, C., Vereecken, L., and Lelieveld, J.: Hydroxyl radical buffered by isoprene oxidation over tropical forests, Nat. Geosci., 5, 190–193, 2012.
Turnipseed, A. A., Huey, L. G., Nemitz, E., Stickel, R., Higgs, J., Tanner, D. J., Slusher, D. L., Sparks, J. P., Flocke, F., and Guenther, A.: Eddy covariance fluxes of peroxyacetyl nitrates (PANS) and NO_y to a coniferous forest, J. Geophys. Res.-Atmos., 111, D09304, doi:10.1029/2005jd006631, 2006.
Warneck, P. and Zerbach, T.: Synthesis of peroxyacetyl nitrate in air by acetone photolysis, Environ. Sci. Technol., 26, 74–79, doi:10.1021/es00025a005, 1992.
Williams, J., Crowley, J., Fischer, H., Harder, H., Martinez, M., Petäjä, T., Rinne, J., Bäck, J., Boy, M., Dal Maso, M., Hakala, J., Kajos, M., Keronen, P., Rantala, P., Aalto, J., Aaltonen, H., Paatero, J., Vesala, T., Hakola, H., Levula, J., Pohja, T., Herrmann, F., Auld, J., Mesarchaki, E., Song, W., Yassaa, N., Nölscher, A., Johnson, A. M., Custer, T., Sinha, V., Thieser, J., Pouvesle, N., Taraborrelli, D., Tang, M. J., Bozem, H., Hosaynali-Beygi, Z., Axinte, R., Oswald, R., Novelli, A., Kubistin, D., Hens, K., Javed, U., Trawny, K., Breitenberger, C., Hidalgo, P. J., Ebben, C. J., Geiger, F. M., Corrigan, A. L., Russell, L. M., Ouwersloot, H. G., Vilà-Guerau de Arellano, J., Ganzeveld, L., Vogel, A., Beck, M., Bayerle, A., Kampf, C. J., Bertelmann, M., Köllner, F., Hoffmann, T., Valverde, J., González, D., Riekkola, M.-L., Kulmala, M., and Lelieveld, J.: The summertime Boreal forest field measurement intensive (HUMPPA-COPEC-2010): an overview of meteorological and chemical influences, Atmos. Chem. Phys., 11, 10599–10618, doi:10.5194/acp-11-10599-2011, 2011.
Wolfe, G. M., Thornton, J. A., McNeill, V. F., Jaffe, D. A., Reidmiller, D., Chand, D., Smith, J., Swartzendruber, P., Flocke, F., and Zheng, W.: Influence of trans-Pacific pollution transport on acyl peroxy nitrate abundances and speciation at Mount Bachelor Observatory during INTEX-B, Atmos. Chem. Phys., 7, 5309–5325, doi:10.5194/acp-7-5309-2007, 2007.
Wolfe, G. M., Thornton, J. A., Yatavelli, R. L. N., McKay, M., Goldstein, A. H., LaFranchi, B., Min, K.-E., and Cohen, R. C.: Eddy covariance fluxes of acyl peroxy nitrates (PAN, PPN and MPAN) above a Ponderosa pine forest, Atmos. Chem. Phys., 9, 615–634, doi:10.5194/acp-9-615-2009, 2009.
Wu, Z., Wang, X., Turnipseed, A. A., Chen, F., Zhang, L., Guenther, A. B., Karl, T., Huey, L. G., Niyogi, D., Xia, B., and Alapaty, K.: Evaluation and improvements of two community models

ACPD
12, 20181–20207, 2012

in simulating dry deposition velocities for peroxyacetyl nitrate (PAN) over a coniferous forest, J. Geophys. Res., 117, D04310, doi:10.1029/2011jd016751, 2012.

Zhang, X., Chen, Z. M., He, S. Z., Hua, W., Zhao, Y., and Li, J. L.: Peroxyacetic acid in urban and rural atmosphere: concentration, feedback on PAN-NO_x cycle and implication on radical chemistry, Atmos. Chem. Phys., 10, 737–748, doi:10.5194/acp-10-737-2010, 2010.

Zheng, W., Flocke, F. M., Tyndall, G. S., Swanson, A., Orlando, J. J., Roberts, J. M., Huey, L. G., and Tanner, D. J.: Characterization of a thermal decomposition chemical ionization mass spectrometer for the measurement of peroxy acyl nitrates (PANs) in the atmosphere, Atmos. Chem. Phys., 11, 6529–6547, doi:10.5194/acp-11-6529-2011, 2011.

ACPD

12, 20181–20207, 2012

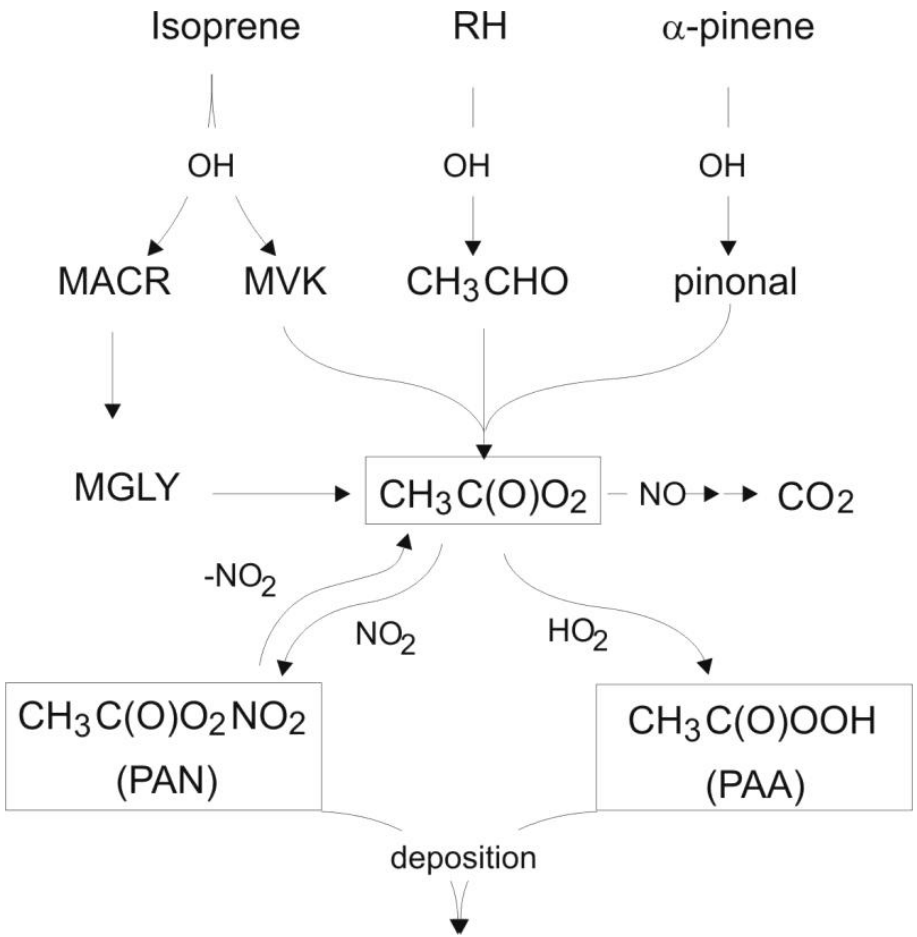

Fig. 1. Exemplary reaction scheme ilustrating the production of the peroxyacetyl radical (PA) from a number of VOC oxidation pathways.

ACPD
12, 20181–20207, 2012

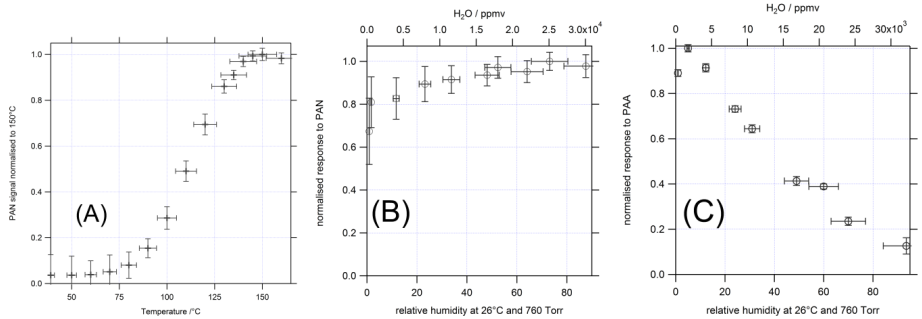

Fig. 2. (A) The dependence of the MPI ICIMS detection of PAN at *m/z* 59 as function of thermal dissociation temperature. The uncertainty in the PAN signal is 1σ and is a function of both the total signal and the subtraction of the background from the PAN source. The uncertainty in the temperature is given as 5 %. **(B)** The normalised response of PAN vesus the relative humidity of the air sample. **(C)** The normalised response to PAA versus the relative humidity of the air sample. Uncertainty of the signal at *m/z* 59 is shown as 1σ and the uncertainty in relative humidity is 10 %.

ACPD
12, 20181–20207, 2012

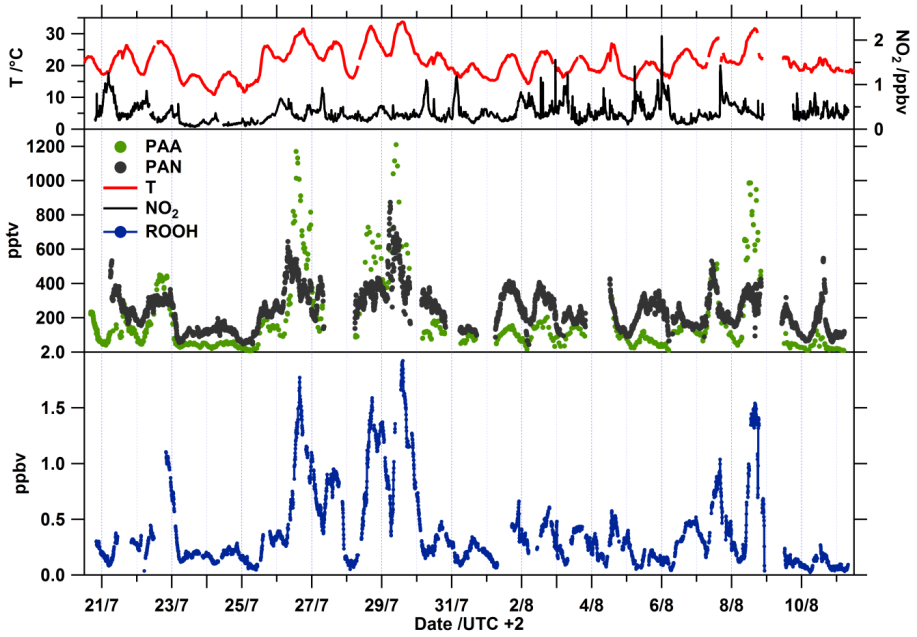

Fig. 3. Time series of PAN, and PAA and organic peroxides (ROOH) from HUMPPA-COPEC along with (top panel) NO_2 mixing ratios and temperature.

ACPD
12, 20181–20207, 2012

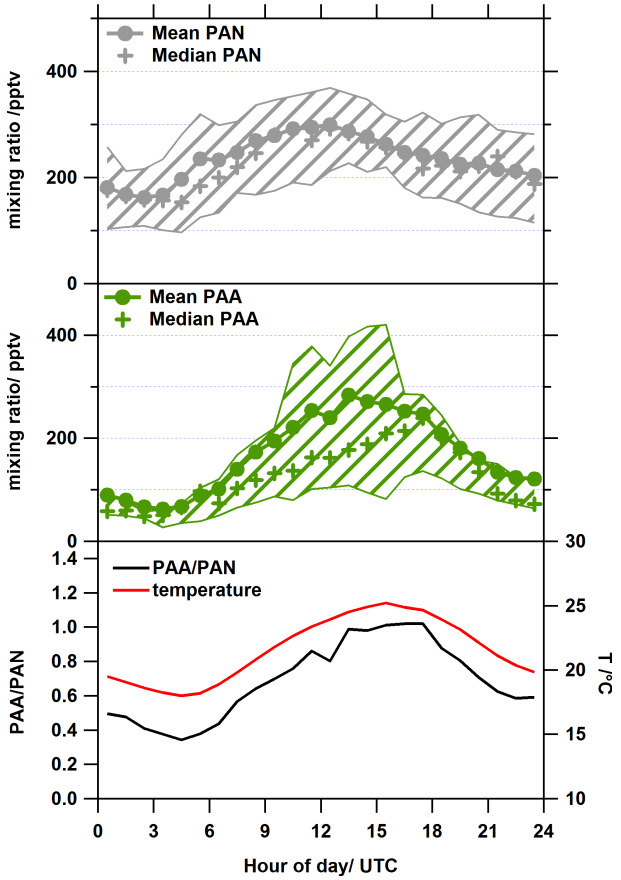

Fig. 4. Diel PAN (top panel) and PAA (middle panel) profiles during HUMPPA-COPEC-2010. The range (25–75th percentile) is indicated by the hatched area. The bottom panel shows the diel PAA-to-PAN ratio alongside the diel temperature during the campaign.

ACPD
12, 20181–20207, 2012

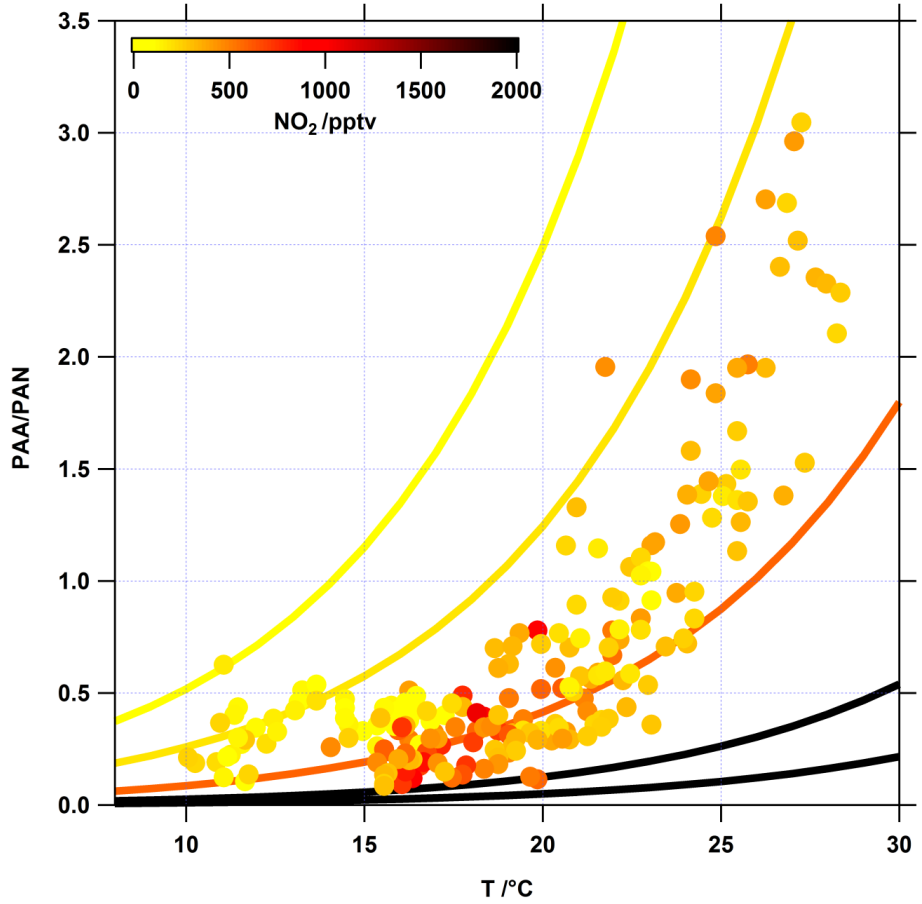

Fig. 5. The relationship between the HUMPPA-COPEC PAA/PAN ratio and temperature. The solid lines are calculations of the ratio based on Eq. (2) at mixing ratios of NO_2 corresponding to 0.1, 0.2, 0.6, 2, and 5 ppbv.

ACPD
12, 20181–20207, 2012

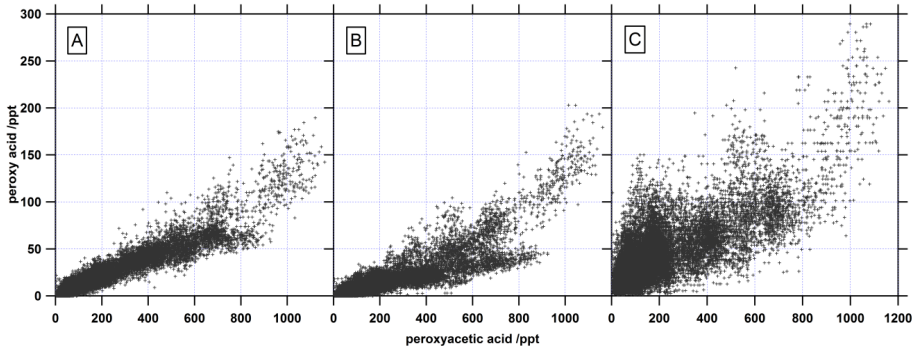

Fig. 6. Relationship between **(A)** PPA vs. PAA, **(B)** PBA vs. PAA, and **(C)** MPA vs. PAA for all data during HUMPPA-COPEC assuming the same instrument sensitivity for all acids as measured for PAA.

ACPD
12, 20181–20207, 2012